

## REPORT

# A homeostatic model of I $\kappa$ B metabolism to control constitutive NF- $\kappa$ B activity

Ellen L O'Dea<sup>1</sup>, Derren Barken<sup>1</sup>, Raechel Q Peralta<sup>1,3</sup>, Kim T Tran<sup>1,4</sup>, Shannon L Werner<sup>1</sup>, Jeffrey D Kearns<sup>1</sup>, Andre Levchenko<sup>2</sup> and Alexander Hoffmann<sup>1,\*</sup>

<sup>1</sup> Signaling Systems Laboratory, Department of Chemistry and Biochemistry, UCSD, La Jolla, CA, USA and <sup>2</sup> Department of Biomedical Engineering, Johns Hopkins University, Baltimore, MD, USA

<sup>3</sup> Present address: Department of Molecular Biology and Biochemistry, UCI, Irvine, CA 92697, USA

<sup>4</sup> Present address: 647 Lincoln Way, San Francisco, CA 94122, USA

\* Corresponding author. Signaling Systems Laboratory, Department of Chemistry and Biochemistry, University of California, San Diego, 9500 Gilman Dr, La Jolla, CA 92037, USA. Tel.: +1 858 822 4670; Fax: +1 858 822 4671; E-mail: ahoffmann@ucsd.edu

Received 4.12.06; accepted 12.3.07

**Cellular signal transduction pathways are usually studied following administration of an external stimulus. However, disease-associated aberrant activity of the pathway is often due to misregulation of the equilibrium state. The transcription factor NF- $\kappa$ B is typically described as being held inactive in the cytoplasm by binding its inhibitor, I $\kappa$ B, until an external stimulus triggers I $\kappa$ B degradation through an I $\kappa$ B kinase-dependent degradation pathway. Combining genetic, biochemical, and computational tools, we investigate steady-state regulation of the NF- $\kappa$ B signaling module and its impact on stimulus responsiveness. We present newly measured *in vivo* degradation rate constants for NF- $\kappa$ B-bound and -unbound I $\kappa$ B proteins that are critical for accurate computational predictions of steady-state I $\kappa$ B protein levels and basal NF- $\kappa$ B activity. Simulations reveal a homeostatic NF- $\kappa$ B signaling module in which differential degradation rates of free and bound pools of I $\kappa$ B represent a novel cross-regulation mechanism that imparts functional robustness to the signaling module.**

*Molecular Systems Biology* 8 May 2007; doi:10.1038/msb4100148

*Subject Categories:* metabolic & regulatory networks; signal transduction

*Keywords:* cross-regulation; homeostasis; mathematical modeling; robustness; signaling module

This is an open-access article distributed under the terms of the Creative Commons Attribution License, which permits distribution, and reproduction in any medium, provided the original author and source are credited. This license does not permit commercial exploitation or the creation of derivative works without specific permission.

## Introduction

Cellular signal transduction pathways mediate responses to extracellular and intracellular signals, such as changing environmental and metabolic conditions, pathogen assault, and developmental cues. Many signaling pathways control the activity of transcription factors that regulate cognate target genes (Brivanlou and Darnell, 2002). For immediate early transcriptional responses (not requiring induced synthesis), such regulation may involve the reversible phosphorylation of the transcription factor to induce dimerization or nuclear translocation (e.g. the Stat, IRF, AP-1 transcription factor families). An alternate means of pathway activation involves stabilization of the transcriptional effector, as in the case of the genotoxic response regulator p53, the hypoxia response factor HIF-1 $\alpha$ , or the developmentally regulated coactivator  $\beta$ -catenin. Thus, signaling in response to stimulus involves

alterations of the homeostatic rates of synthesis and degradation found in unstimulated cells.

In contrast, the cellular abundance of the transcription factor NF- $\kappa$ B does not change dramatically during signaling. NF- $\kappa$ B is the critical mediator of cellular responses to a large number of physiological stimuli, including inflammatory cytokines, developmental signals, pathogens, and cellular stresses (Figure 1A) (Hoffmann and Baltimore, 2006). Although inflammatory signaling leads to transient NF- $\kappa$ B activity that is dynamically regulated by feedback mechanisms, elevated constitutive levels of active NF- $\kappa$ B are associated with chronic inflammatory diseases and many types of cancer (Karin, 2006).

NF- $\kappa$ B activity is inhibited by association with the inhibitor proteins, I $\kappa$ B $\alpha$ , I $\kappa$ B $\beta$ , or I $\kappa$ B $\epsilon$ , which mask its nuclear localization sequence and inhibit its DNA-binding activity. The regulated metabolism of I $\kappa$ B proteins—their synthesis and

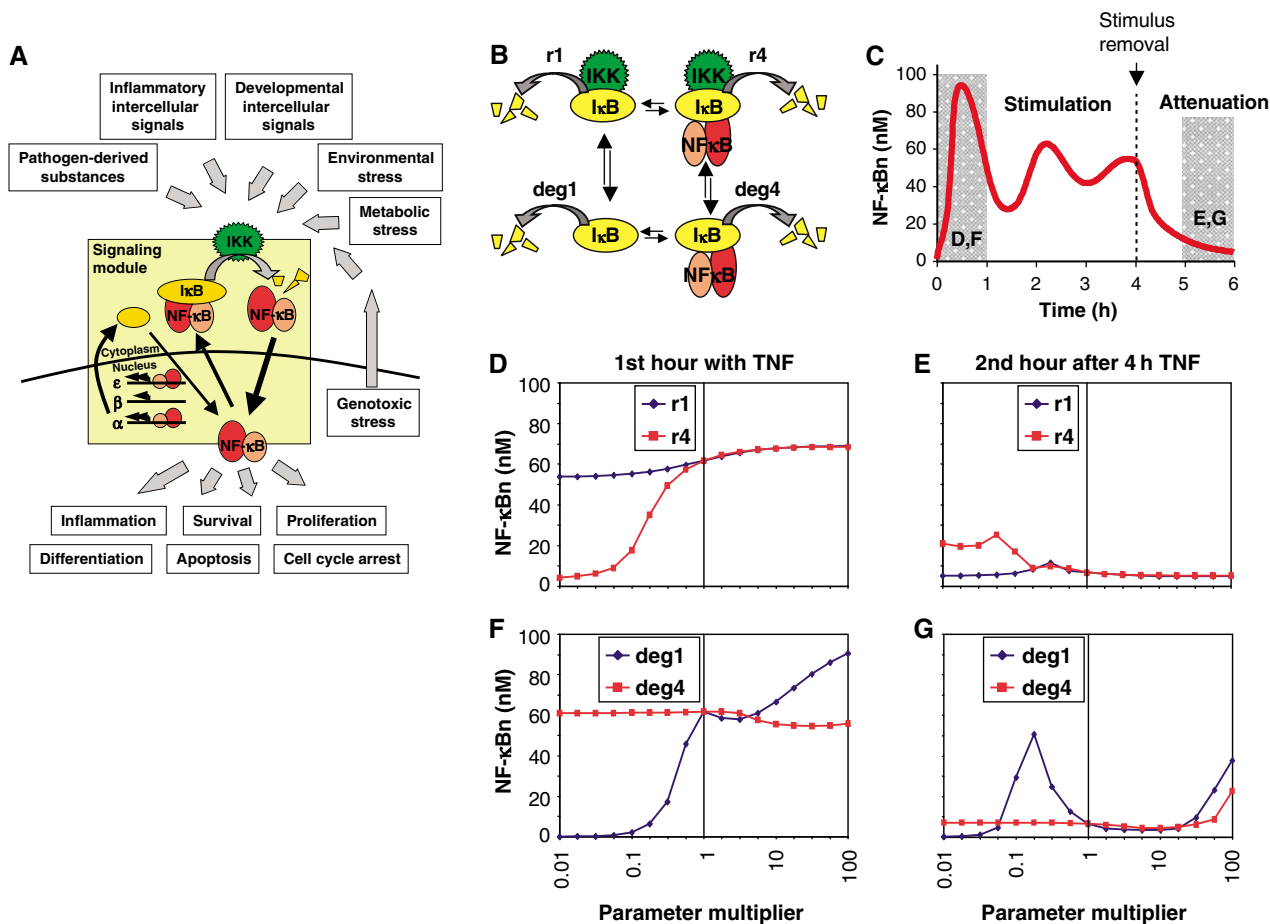


**Figure 1** Exploring the relative importance of I $\kappa$ B degradation mechanisms by computational parameter sensitivity analysis. **(A)** Schematic of the NF- $\kappa$ B signaling module and its physiological importance in the transduction of diverse inflammatory, developmental, and stress signals. **(B)** Illustration of the four I $\kappa$ B degradation pathways within the NF- $\kappa$ B signaling module. deg1 and deg4 are IKK-independent degradation rate constants for free and bound I $\kappa$ B $\alpha$ . r1 and r4 are IKK-dependent degradation rate constants for free and bound I $\kappa$ B $\alpha$ . **(C)** Computational simulation of NF- $\kappa$ B activation over a 6-h time course. TNF stimulation begins at time 0, and is removed at 4 h. Mean activity in the first hour of stimulation and the second hour after removal of the stimulus (shaded in gray) were used to create the plots in (D–F) and (G). **(D–G)** Graphs showing the average nuclear NF- $\kappa$ B (y axis) during the first hour (D, F) or during the second hour after 4 h (E, G) of TNF stimulation for different values (x axis) of the IKK-dependent (D, E) or -independent (F, G) degradation rate constants of free (blue line) and bound (red line) I $\kappa$ B.

degradation—critically controls NF- $\kappa$ B signaling (Ghosh *et al*, 1998). Synthesis of I $\kappa$ B proteins is a highly regulated process, with at least two isoforms, I $\kappa$ B $\alpha$  and I $\kappa$ B $\epsilon$ , being subject to NF- $\kappa$ B-inducible synthesis, thereby providing negative feedback (Scott *et al*, 1993; Kearns *et al*, 2006). Stimulus-induced I $\kappa$ B degradation is controlled by the I $\kappa$ B kinase (IKK), which phosphorylates two N-terminal serines. This leads to I $\kappa$ B polyubiquitination and degradation via the 26S proteasome, thus liberating NF- $\kappa$ B for nuclear translocation (Ghosh *et al*, 1998; Yaron *et al*, 1998).

These processes were described in a mathematical model of the IKK-I $\kappa$ B-NF- $\kappa$ B signaling module to recapitulate NF- $\kappa$ B activation in response to TNF stimulation (Hoffmann *et al*, 2002). Its construction relied on rate constants available in the literature from a diverse set of experiments. As no isoform-specific data were available, rate constants pertaining to I $\kappa$ B $\beta$  and I $\kappa$ B $\epsilon$  were assumed to be the same as those measured for I $\kappa$ B $\alpha$ . Although this model accurately recapitulates NF- $\kappa$ B signaling in response to TNF, in the unstimulated state the

estimated I $\kappa$ B levels were found to be unexpectedly high (Lipniacki *et al*, 2004). In fact, the vast majority of I $\kappa$ B were calculated to be in the free form, contradictory to experimental studies showing that free I $\kappa$ B $\alpha$  accounts for less than 15% of the total cellular I $\kappa$ B (Rice and Ernst, 1993).

Despite our detailed understanding of stimulus-induced NF- $\kappa$ B signaling, there is less clarity about the mechanisms mediating I $\kappa$ B turnover in the absence of external stimulation. Early studies reported that basal turnover of I $\kappa$ B, unlike its induced degradation, does not require the IKK-targeted serines, the C-terminal PEST domain, or poly-ubiquitination of I $\kappa$ B (Krappmann *et al*, 1996), whereas others found robust C-terminal phosphorylation and poly-ubiquitination (Pando and Verma, 2000).

By distinguishing between NF- $\kappa$ B-bound and free I $\kappa$ B pools using an I $\kappa$ B interaction mutant, the half-life of bound I $\kappa$ B was found to be five-fold longer than that of free I $\kappa$ B in unstimulated cells (Pando and Verma, 2000). However, free I $\kappa$ B is a poorer substrate for IKK than NF- $\kappa$ B-bound I $\kappa$ B (Zandi

*et al*, 1998), although it is routinely used as a substrate to measure IKK activity *in vitro*. Free I $\kappa$ B turnover was proposed to involve casein kinase 2 (CK2)-mediated phosphorylation of the C-terminal domain and ubiquitination (Schwarz *et al*, 1996; Bren *et al*, 2000), but others suggested that CK2 is involved in inducible degradation of NF- $\kappa$ B-bound I $\kappa$ B (Kato *et al*, 2003), or that ubiquitination was not required (Krappmann *et al*, 1996; Alvarez-Castelao and Castano, 2005).

Given these contradictory results in the literature, the lack of data on two of the three I $\kappa$ B isoforms, and the poor fit of computational simulations of the NF- $\kappa$ B signaling module in cells not exposed to TNF, we generated genetic tools—mouse knockout cell lines—to isolate cleanly the endogenous-free and -bound I $\kappa$ B protein pools and probe their degradation with kinase knockouts and pharmacological inhibitors. In addition, we used computational modeling (i) to identify which constitutive degradation rate constants play a critical role in determining stimulus responsiveness, (ii) to determine new biochemical rate constants based on our experimental results, (iii) to confirm the validity of the new parameters by simulating the cellular steady state, and (iv) to reveal the control of I $\kappa$ B degradation by NF- $\kappa$ B as a cross-regulatory mechanism.

## Results and discussion

### IKK-dependent and -independent degradation of I $\kappa$ Bs determine NF- $\kappa$ B signaling

Four degradation rate constants govern the *in vivo* half-life of I $\kappa$ B proteins (Figure 1B). An I $\kappa$ B molecule can exist in either the free or NF- $\kappa$ B-bound form. Both forms may be degraded in an IKK-dependent manner (we denote the I $\kappa$ B $\alpha$  rate constants of these processes  $r_1$  and  $r_4$ , respectively), but are also subject to constitutive degradation in an IKK-independent manner (with the rate constants denoted as  $deg_1$  and  $deg_4$ ). These mechanisms are described as first-order rate constants in our mathematical model of NF- $\kappa$ B signaling (Hoffmann *et al*, 2002).

To explore the functional significance of each I $\kappa$ B degradation rate constant in NF- $\kappa$ B signal transduction, we performed simulations of TNF signaling after altering one of the four rate constants (simultaneously for the I $\kappa$ B $\alpha$ ,  $\beta$ , and  $\epsilon$  isoforms) with a parameter multiplier ranging from 0.01 to 100. For each parameter multiplier, we calculated the average nuclear NF- $\kappa$ B level in response to TNF during the early phase (during the first hour of stimulation) and the later attenuation phase (during the second hour after a 4 h stimulation) (Figure 1C). By plotting the calculated NF- $\kappa$ B activity against its parameter multiplier, we can interpret the sensitivity of the system to each rate constant for two critical features of the NF- $\kappa$ B response to a transient TNF stimulus: activation and attenuation of NF- $\kappa$ B activity.

We first examined the impact of changes in IKK-dependent I $\kappa$ B degradation rate constants on NF- $\kappa$ B activation. During the first hour of TNF stimulation, the amount of nuclear NF- $\kappa$ B calculated by the model is fairly insensitive to even drastic changes in the IKK-dependent degradation rate of free I $\kappa$ B (Figure 1D, blue line). In contrast, slowing down the IKK-induced degradation of NF- $\kappa$ B-bound I $\kappa$ B severely dampens

NF- $\kappa$ B activity (Figure 1D, red line). During the attenuation phase, the amount of nuclear NF- $\kappa$ B predicted by the model was similarly found to be insensitive to changes in IKK-dependent degradation of free I $\kappa$ B (Figure 1E, blue line), but slowing the IKK-dependent degradation rate of bound I $\kappa$ B results in a loss of attenuation (Figure 1E, red line).

The IKK-independent I $\kappa$ B degradation rates control the stimulus-independent turnover of I $\kappa$ B proteins, and thus maintain a resting state equilibrium of I $\kappa$ B levels. Examining whether these IKK-independent degradation rates play a role in determining the cellular responsiveness to inflammatory stimuli revealed that during the first hour of TNF stimulation the signaling module is dramatically more sensitive to the basal turnover rate of free I $\kappa$ B (Figure 1F, blue line) than of bound I $\kappa$ B (Figure 1F, red line). Furthermore, our simulations predicted that a more stable free I $\kappa$ B results in a loss of attenuation, whereas the basal turnover rate of the bound I $\kappa$ Bs had no effect (Figure 1G).

In sum, our computational simulations revealed that two of the four possible degradation pathways play a particularly important role in controlling NF- $\kappa$ B signaling. Whereas much is known about the stimulus-responsive IKK-mediated degradation pathway, the IKK-independent degradation mechanism of free I $\kappa$ B has received surprisingly little experimental attention. Given the importance of these degradation rate constants in our computational analysis, we set out to examine them in more detail experimentally.

### NF- $\kappa$ B regulation of I $\kappa$ B protein turnover and synthesis

To measure experimentally *in vivo* degradation rate constants for NF- $\kappa$ B-bound I $\kappa$ B proteins, we used the ribosomal inhibitor cycloheximide (CHX) to reduce the synthesis of new I $\kappa$ B proteins (by 85%; Supplementary Figure S1A), and examined the amount of nuclear NF- $\kappa$ B DNA-binding activity via electrophoretic mobility shift assay (EMSA). Treatment of wild-type MEFs with CHX over a 60 h time course induced nuclear NF- $\kappa$ B activity that corresponds to 25–35% of peak TNF-induced NF- $\kappa$ B activity (Figure 2A, Supplementary Figure S1B). To determine the relative contributions of each NF- $\kappa$ B-bound I $\kappa$ B isoform ( $\alpha$ ,  $\beta$ , and  $\epsilon$ ) to CHX-mediated NF- $\kappa$ B activation, we used a panel of I $\kappa$ B double-knockout MEFs, which contain only one I $\kappa$ B isoform. These cells were previously used to determine the degradation rate constants for each I $\kappa$ B isoform by TNF-induced NF- $\kappa$ B activation, which revealed that upon IKK activation, I $\kappa$ B $\alpha$  was degraded most rapidly, followed by I $\kappa$ B $\epsilon$ , and then I $\kappa$ B $\beta$  (Hoffmann *et al*, 2002). Interestingly, we find the same trend in stimulus-independent degradation, where I $\kappa$ B $\beta$  is the most stable and I $\kappa$ B $\alpha$  is the least stable (Figure 2B and Supplementary Figure S1C).

To investigate the stability of the unbound, or 'free', I $\kappa$ B proteins in resting cells, we generated *crel*<sup>-/-</sup>*rela*<sup>-/-</sup>*nfkb1*<sup>-/-</sup> (termed '*nfkb*<sup>-/-</sup>') MEFs deficient in the three NF- $\kappa$ B proteins known to interact with the classical I $\kappa$ B proteins: RelA, c-Rel, and p50. Western blots revealed a dramatic reduction in the amount of total I $\kappa$ B protein level in these cells compared to wild type (Figure 2C, compare lanes 3 and 6). A dilution series

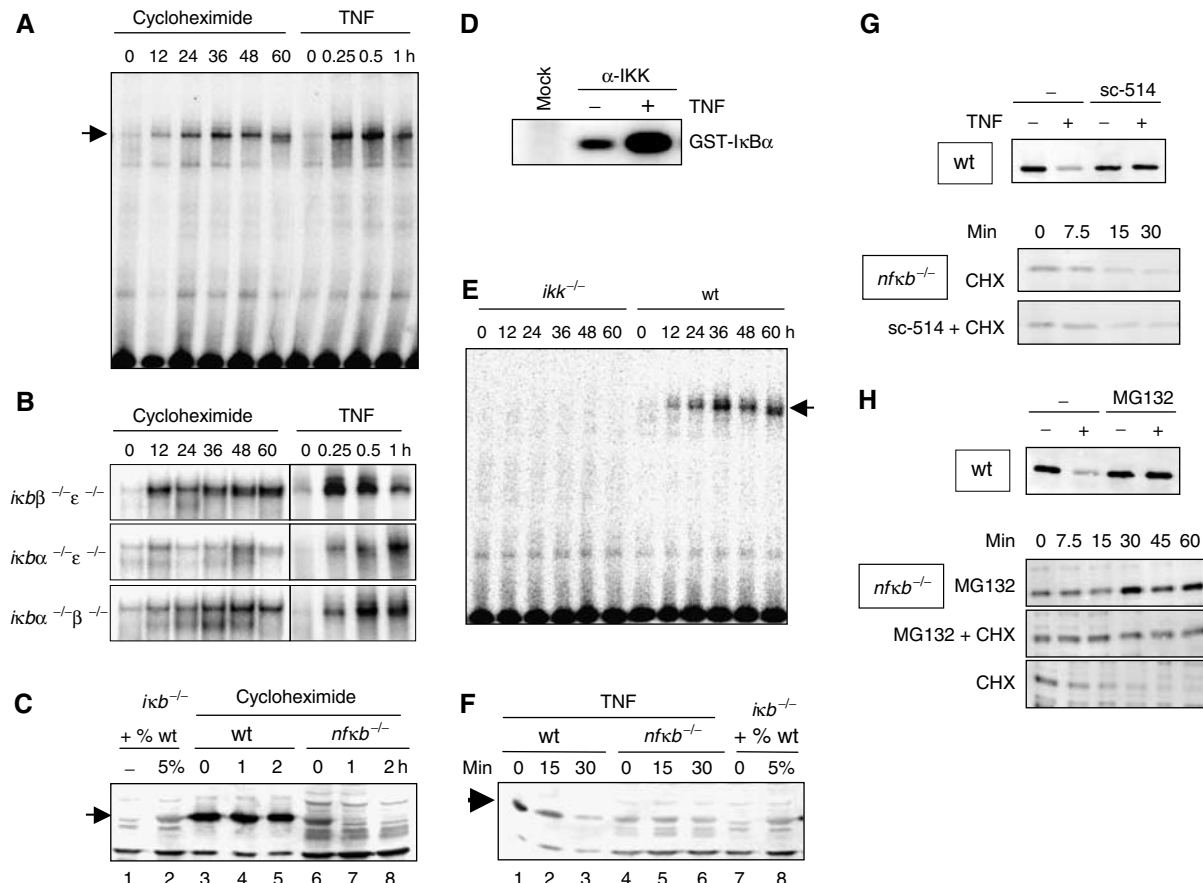


**Figure 2** Experimental studies of degradation pathways of NF- $\kappa$ B-bound and -free I $\kappa$ B proteins. **(A)** NF- $\kappa$ B activity as measured by EMSA of nuclear extracts from wild-type cells treated with 10  $\mu$ g/ml CHX or 1 ng/ml TNF for indicated times. **(B)** NF- $\kappa$ B activity as measured by EMSA of nuclear extracts from *ikb $\beta$ <sup>-/-</sup> $\epsilon$ <sup>-/-</sup>*, *ikb $\alpha$ <sup>-/-</sup> $\epsilon$ <sup>-/-</sup>*, or *ikb $\alpha$ <sup>-/-</sup> $\beta$ <sup>-/-</sup>* cells treated with 10  $\mu$ g/ml CHX or 1 ng/ml TNF. **(C)** Western blot for I $\kappa$ B $\alpha$  in CHX-treated wild-type and *nf $\kappa$ b<sup>-/-</sup>* cells. The first two lanes show *ikb $\alpha$ <sup>-/-</sup> $\beta$ <sup>-/-</sup> $\epsilon$ <sup>-/-</sup>* extract and *ikb $\alpha$ <sup>-/-</sup> $\beta$ <sup>-/-</sup> $\epsilon$ <sup>-/-</sup>* extract mixed with 5% wild-type extract to show the protein level of I $\kappa$ B $\alpha$  in the *nf $\kappa$ b<sup>-/-</sup>* cells was approximately 5% that in the wild-type cells at time zero. **(D)** Cytoplasmic extracts of wild-type cells were immunoprecipitated with IKK $\gamma$  antibody and subject to an *in vitro* kinase assay. In the 'mock' lane, no antibody was added during the IP. **(E)** NF- $\kappa$ B activity as measured by EMSA of nuclear extracts from *ikk $\alpha$ <sup>-/-</sup> $\beta$ <sup>-/-</sup>* or wild-type MEFs treated with 10  $\mu$ g/ml CHX. **(F)** Western blot for I $\kappa$ B $\alpha$  of protein extracts from TNF (1 ng/ml)-treated wild-type or *rela<sup>-/-</sup>crel<sup>-/-</sup>nf $\kappa$ b1<sup>-/-</sup>* cells. **(G)** Western blots for I $\kappa$ B $\alpha$  of protein extracts from TNF-treated wild-type cells (top panel) in the presence or absence of the IKK-inhibitor sc-514. Bottom panels show Western blots for I $\kappa$ B $\alpha$  of protein extracts from CHX (10  $\mu$ g/ml)-treated cells in the presence or absence of sc-514. **(H)** Western blots for I $\kappa$ B $\alpha$  of protein extracts from wild-type cells treated with TNF $\alpha$  (1 ng/ml) with or without the presence of the proteasome inhibitor MG132 (top panel). Western blots for I $\kappa$ B $\alpha$  of protein extracts from *nf $\kappa$ b<sup>-/-</sup>* cells treated with 10  $\mu$ g/ml CHX, 10  $\mu$ M MG132, or both.

of wild-type protein extract with *ikb $\alpha$ <sup>-/-</sup> $\beta$ <sup>-/-</sup> $\epsilon$ <sup>-/-</sup>* extract showed that the amount of I $\kappa$ B $\alpha$  in the *nf $\kappa$ b<sup>-/-</sup>* cells was approximately one-twentieth the amount in wild-type cells, and that this ratio is probably even lower for I $\kappa$ B $\beta$  and I $\kappa$ B $\epsilon$  (Supplementary Figure S2A). No decrease in I $\kappa$ B levels was detected in MEFs deficient in the NF- $\kappa$ B proteins RelB and *nf $\kappa$ b2* p52, which are non-canonical NF- $\kappa$ B proteins that do not bind canonical I $\kappa$ B proteins.

Strikingly, the level of I $\kappa$ B $\alpha$  mRNA in the *nf $\kappa$ b<sup>-/-</sup>* cells was only two-fold lower than in wild type, with even smaller differences in I $\kappa$ B $\beta$  and I $\kappa$ B $\epsilon$  mRNA levels (Supplementary Figure S2B), suggesting that differential protein stability may account for different I $\kappa$ B protein levels in wild-type and *nf $\kappa$ b<sup>-/-</sup>* cells. Indeed, treating *nf $\kappa$ b<sup>-/-</sup>* cells with CHX resulted in rapid decreases of I $\kappa$ B $\alpha$  protein, whereas it remains stable in the wild-type cells beyond 2 h (Figure 2C). These results suggest that NF- $\kappa$ B has a regulatory role not only in controlling I $\kappa$ B $\alpha$  transcription, but also in stabilizing I $\kappa$ B proteins.

We next investigated whether the dramatically different half-life of free and bound I $\kappa$ B proteins may be due to different mechanisms governing their degradation.

IKK phosphorylation is a key mediator of the stimulus-induced degradation of NF- $\kappa$ B-bound I $\kappa$ B proteins, yet it is unclear if and how IKK may participate in the basal degradation of bound I $\kappa$ B. We first performed a kinase assay to examine the IKK activity of immunoprecipitated IKK complex from wild-type MEFs. Surprisingly, even in resting cells, a substantial amount of basal activity associated with the IKK complex was detectable (Figure 2D). In cells lacking the IKK catalytic subunits, IKK $\alpha$  and IKK $\beta$ , no activation of NF- $\kappa$ B upon CHX treatment (Figure 2E) was observed, indicating that IKK-dependent phosphorylation is required for the basal turnover of NF- $\kappa$ B-bound I $\kappa$ B proteins.

We sought to determine if IKK activity is involved in the turnover of free I $\kappa$ B proteins as well. IP-IKK kinase assays determined that the basal and inducible IKK activities are

**Table I** Rate constants for IKK-independent IκB degradation: a role for NF-κB

	Rate constants (s <sup>-1</sup> )	NF-κB effect
IκBα		
Free	deg1:2 × 10 <sup>-3</sup>	2000
Bound	deg4:1 × 10 <sup>-6</sup>	
IκBβ		
Free	deg2:3 × 10 <sup>-3</sup>	3000
Bound	deg5:1 × 10 <sup>-6</sup>	
IκBε		
Free	deg3:3 × 10 <sup>-3</sup>	3000
Bound	deg6:1 × 10 <sup>-6</sup>	

New rate constants governing the uninduced IKK-independent degradation of IκB proteins derived from experiments in this paper and used in an updated version of the mathematical model. The ratio of IκB degradation rate constants in the presence and absence of NF-κB is defined as the 'NF-κB effect'.

intact in the *nfkb*<sup>-/-</sup> cell line (Supplementary Figure S3A). Treatment of wild-type cells with TNF led to the rapid degradation of IκBα, but did not affect the levels of IκBα in the *nfkb*<sup>-/-</sup> cells (Figure 2F and Supplementary Figure S3B), suggesting that the inducible IKK activity is not involved in the degradation of free IκBα. Further, the IKK inhibitor, sc-514, which diminishes the TNF-induced degradation of IκBα in wild-type cells, did not have an effect on the basal turnover of free IκB in *nfkb*<sup>-/-</sup> cells (Figure 2G). In contrast, the proteasome inhibitor MG132 prevented not only TNF-induced degradation of IκBα in wild-type cells, but also led to accumulation of free IκB in *nfkb*<sup>-/-</sup> cells, and prevented its degradation when cells were cotreated with CHX (Figure 2H).

Based on our new biochemical data, we revised the parameter values governing degradation of IκB proteins within the NF-κB signaling module and incorporated these into our mathematical model (now termed model 1.1). Half-lives for free IκB proteins were determined to be 5–10 min (Figures 2H and Supplementary Figure S2, allowing us to calculate the respective first order rate constants (deg1-3). Our data highly constrained IKK-independent degradation rate constants (deg4-6) for NF-κB-bound IκB proteins (Figure 2E). While previous studies suggested that NF-κB stabilized free IκB degradation by a factor of 5 (Pando and Verma, 2000), our new measurements (Table I) indicate an NF-κB effect of 2000-fold with respect to the IKK-independent degradation of IκB proteins. This large discrepancy likely lies in the facts that (i) we have used a clean genetic system to isolate free endogenous IκB from NF-κB proteins, and have thus obtained a much faster degradation rate for free IκB and (ii) we have determined that degradation of NF-κB-bound IκB proteins can only occur through an IKK-involving mechanism and have thus drastically decreased the IKK-independent degradation rate of bound IκB.

After incorporation of the new rate constants in Table I, we performed model fitting as described previously (Hoffmann *et al*, 2002) to obtain new degradation rate constants for IKK-induced degradation of NF-κB-bound IκB proteins (r4-6; Supplementary Table SI). As IKK-mediated phosphorylation of IκB is five-fold more efficient when NF-κB is present (Zandi *et al*, 1998), we divided the newly determined r4-6 by 5 to determine IKK-induced degradation of free IκB proteins

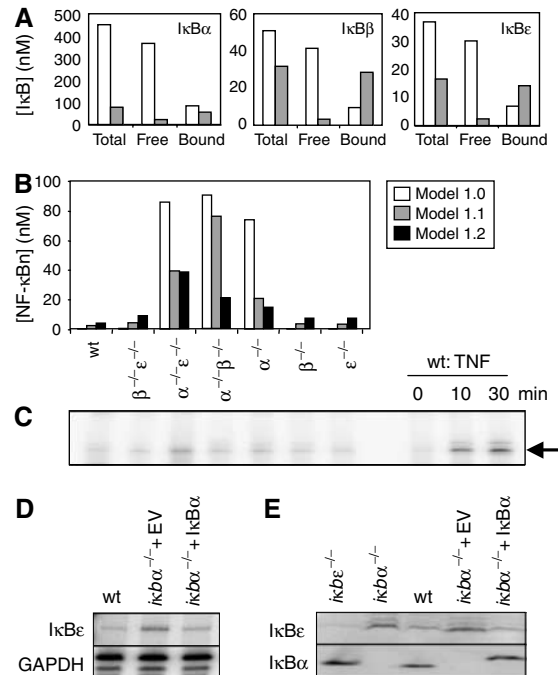


**Figure 3** An improved model of the homeostatic NF-κB signaling module. **(A)** Model calculations of IκBα, β, and ε protein levels (nM) in unstimulated cells for total IκB, free IκB, or NF-κB-bound IκB. Model 1.0 predictions are white bars, model 1.1 predictions are gray bars. **(B)** Model calculations of NF-κB activity (nM) in unstimulated wild-type and *ikb*<sup>-/-</sup> cells predicted by model version 1.0 (white bars), version 1.1 (gray bars), and version 1.2 (black bars). **(C)** NF-κB activity in untreated cells as measured by EMSA of nuclear extracts from the *ikb*<sup>-/-</sup> cell genotype labeled above each lane. The last three lanes are controls for the NF-κB band and are nuclear extracts from wild-type cells treated with TNF (1 ng/ml). **(D)** RNase protection assay showing levels of IκBε mRNA in untreated wild-type cells, *ikbα*<sup>-/-</sup> cells with empty vector control, or *ikbα*<sup>-/-</sup> cells expressing a retroviral *ikbα* transgene. GAPDH is used as a loading control. **(E)** Western blots for IκBε and IκBα in resting cells. The cell genotype is listed above each lane.

(Supplementary Table SI, see Supplementary information for rate constant derivations). Including eight-fold differential IKK association rate constants (Zandi *et al*, 1998), the combined NF-κB effect on IKK-mediated degradation of free and bound IκB proteins is almost 50-fold.

Our results emphasize that NF-κB determines the degradation mechanism of IκB proteins. When bound to NF-κB, IκB turnover is slow and dependent on the basal activity of IKK. In contrast, when not bound to NF-κB, IκB degradation is rapid and independent of IKK activity.

### Cross-regulation between IκB proteins via half-life control by NF-κB

We compared the steady-state levels of IκB predicted for unstimulated cells by the previous version of the model (referred to as model 1.0) (Hoffmann *et al*, 2002) and the new version of the model that incorporates the new rate constants of Tables I and Supplementary Table I (model 1.1) (Figure 3A, white and gray bars, respectively). The new degradation rate constants result in predictions of a much smaller pool of free IκB protein, as well as less total cellular IκB protein. The

simulation results produced with the new model (1.1) are therefore in much better agreement with experimental observations (Rice and Ernst, 1993) than those with the previous model. Although a previous study (Lipniacki *et al*, 2004) lowered the I $\kappa$ B synthesis rate to correct the model-predicted ratio of free to bound I $\kappa$ B protein in the steady state, our new data indicate that the rapid free I $\kappa$ B degradation necessitates a high synthesis rate.

Next, we examined the consequences of the new degradation parameters on constitutive NF- $\kappa$ B activity in a series of I $\kappa$ B knockout cell lines. The previous model predicts that the removal of I $\kappa$ B $\alpha$  results in high levels of nuclear NF- $\kappa$ B activity in unstimulated cells (Figure 3B), which does not match with our experimental observations (Figure 3C). The differential degradation rates of bound and unbound I $\kappa$ B protein may result in molecular compensation among the I $\kappa$ B isoforms; upon deletion of a single I $\kappa$ B isoform, the newly available NF- $\kappa$ B may act to stabilize the remaining I $\kappa$ B isoforms, resulting in the cytoplasmic retention of NF- $\kappa$ B. Indeed, model 1.1 predicts a lower level of NF- $\kappa$ B activity in unstimulated knockout cells than version 1.0 (Figure 3B, compare white and gray bars). EMSA results (Figure 3C) confirm the new predictions, indicating that functional I $\kappa$ B compensation via differential half-life control indeed exists.

In the case of *ikb $\alpha$ <sup>-/-</sup> $\beta$ <sup>-/-</sup>* cells where I $\kappa$ B $\epsilon$  is the only isoform present, our model predicts a markedly higher level of NF- $\kappa$ B activity than seen experimentally. However, we have recently characterized an NF- $\kappa$ B-inducible I $\kappa$ B $\epsilon$  mRNA synthesis mechanism (Kearns *et al*, 2006). Incorporation of this feedback mechanism into the model (referred to as model 1.2) indeed lowers the predicted basal NF- $\kappa$ B levels (Figure 3B, black bars) to levels that are in good agreement with the EMSA results. We measured I $\kappa$ B $\epsilon$  mRNA levels and found that they are indeed upregulated in *ikb $\alpha$ <sup>-/-</sup>* cells compared to wild type (Figure 3D), resulting in higher I $\kappa$ B $\epsilon$  protein levels (Figure 3E). To determine whether this effect was the result of homeostatic regulation within the NF- $\kappa$ B signaling module, we used a retroviral transgene to reconstitute I $\kappa$ B $\alpha$  expression in *ikb $\alpha$ <sup>-/-</sup>* cells. Indeed, we found that I $\kappa$ B $\epsilon$  upregulation was reversible, confirming that even in resting cells constitutive NF- $\kappa$ B activity plays a role in transcriptional regulation of its inhibitors to control its own steady-state activity.

## Homeostatic control via distinct I $\kappa$ B degradation pathways

Our analysis of the NF- $\kappa$ B signaling module in unstimulated cells reveals a highly dynamic homeostatic state that is controlled by multiple synthesis and degradation mechanisms of the regulatory I $\kappa$ B proteins. As such we find that NF- $\kappa$ B itself has two roles in regulating its own basal activity. NF- $\kappa$ B binding to I $\kappa$ B proteins removes them from this rapid degradation pathway, and sensitizes them to a slow degradation mechanism that is dependent on basal IKK activity. Second, constitutive NF- $\kappa$ B activity also impacts transcription rates of I $\kappa$ B $\alpha$  and I $\kappa$ B $\epsilon$ , thus providing for negative feedback even in the absence of an external stimulus.

Our studies identify the free I $\kappa$ B protein degradation pathway as a major determinant of constitutive NF- $\kappa$ B and of

stimulus responsiveness of the NF- $\kappa$ B signaling module. Given this hitherto unappreciated importance, determining the enzymatic and potentially regulatory mechanisms of the free I $\kappa$ B degradation pathway is critical for understanding the regulation of NF- $\kappa$ B in diverse physiological and pathological settings.

Owing to the dynamic nature of the I $\kappa$ B-NF- $\kappa$ B equilibrium, the majority of newly synthesized I $\kappa$ B is likely degraded before ever binding NF- $\kappa$ B. However, this is not unlike other signal transduction pathways that consume significant cellular resources for the maintenance of a dynamic homeostatic state. For example, the transcription factors p53, HIF-1 $\alpha$ , and  $\beta$ -catenin are continually synthesized and degraded. Upon signaling, the respective degradation pathways are inhibited to allow for their nuclear accumulation and function (Ivan *et al*, 2001; Jaakkola *et al*, 2001; Moon, 2005). How may this energy-consuming process of maintaining a dynamic homeostasis benefit the cell? Future computational studies may suggest that homeostatic control of the NF- $\kappa$ B signaling module confers sensitivity to signals but ensures a very steady low equilibrium activity that is less likely to drift (D Barken, unpublished results). In addition, combined computational and experimental studies may demonstrate that such a dynamic equilibrium state sensitizes the signaling pathway to metabolic changes, such that stress conditions constitute an input signal that results in cellular responses (Ellen L O'Dea, unpublished results).

## Materials and methods

### Cells and reagents

Primary and 3T3 immortalized MEF were generated from E12.5–14.5 embryos and maintained as described previously (Hoffmann *et al*, 2002). *rela<sup>-/-</sup>crel<sup>-/-</sup>nfkb1<sup>-/-</sup>* MEFs were generated from E12.5-timed matings of *rela<sup>+/-</sup>crel<sup>-/-</sup>nfkb1<sup>-/-</sup>* mice and *ikb $\alpha$ <sup>-/-</sup> $\beta$ <sup>-/-</sup> $\epsilon$ <sup>-/-</sup>* cells will be described elsewhere. *ikk1<sup>-/-</sup>ikk2<sup>-/-</sup>* cells were a kind gift from Inder Verma. *ikb $\alpha$ <sup>-/-</sup>* MEF lines reconstituted with pBabe-I $\kappa$ B $\alpha$  and empty vector control were a generous gift from Erika Mathes. Recombinant murine TNF was from Roche; CHX, sc-514, and MG132 from Sigma. RelA/p65 (sc-372), RelB (sc-226), cRel (sc-71), I $\kappa$ B $\alpha$  (sc-371), I $\kappa$ B $\beta$  (sc-946), and I $\kappa$ B $\epsilon$  (sc-7156) antibodies were from Santa Cruz Biotechnology. Trans-<sup>35</sup>S-methionine label was from MP Biomedicals.

### Biochemical analysis

Whole-cell extracts were prepared in RIPA buffer and equivalent protein amounts subjected to immunoblot analysis using ECL-plus (Amersham/GE Healthcare). Nuclear extracts were prepared and used for electrophoretic EMSA as described (Hoffmann *et al*, 2002). Immunoprecipitation kinase assay performed as in Werner *et al* (2005). Signals were quantified using a phosphorimager (Molecular Dynamics) and ImageQuant software version 5.2 (GE Healthcare). Dilution series with knockout extracts assured that Western blot signals were in the linear range. Total cellular RNA was isolated with Trizol reagent (Invitrogen) and used for RNase protection assay as described in Kearns *et al* (2006).

Cells were labeled with 200  $\mu$ Ci/ml <sup>35</sup>S-methionine label for indicated times. Whole-cell extracts were prepared in RIPA buffer and dried on filter paper. <sup>35</sup>S-Met incorporation was measured by scintillation count and CHX-treated cells versus untreated cells were compared to measure the percentage of translational inhibition.

## Computational modeling

The mathematical model of the IKK-I $\kappa$ B-NF- $\kappa$ B signaling module was described in Hoffmann *et al* (2002). This model (version 1.0) was used to generate Figure 1. Model version 1.1 includes the parameter values shown in Table I and baseline level of IKK of 1 nM. Simulations were performed in Matlab and Excel as described previously (Hoffmann *et al*, 2002) with extended equilibration times. A complete list of the parameter values can be found in the Supplementary information. Graphs were generated in Excel. The Matlab code file is available upon request, and the SBML code is available at the MSB website.

## Supplementary information

Supplementary information is available at the *Molecular Systems Biology* website ([www.nature.com/msb](http://www.nature.com/msb)).

## Acknowledgements

We thank Erika Mathes, Gouri Ghosh, and Betsy Komives for insightful discussions, and Gouri Ghosh for critical reading of the manuscript. We are grateful to Santa Cruz Biotechnology for antibodies. EO is supported by the Heme Training Grant, JDK by the Molecular Biophysics Training Grant, DB by the UCSD Bioinformatics Graduate Training Grant, and SLW by an NSF Graduate Fellowship. This study was supported by NIH grants GM72024, GM69013, and GM071573.

## References

- Alvarez-Castelao B, Castano JG (2005) Mechanism of direct degradation of I $\kappa$ B $\alpha$  by 20S proteasome. *FEBS Lett* **579**: 4797–4802
- Bren GD, Pennington KN, Paya CV (2000) PKC-zeta-associated CK2 participates in the turnover of free I $\kappa$ B $\alpha$ . *J Mol Biol* **297**: 1245–1258
- Brivanlou AH, Darnell Jr JE (2002) Signal transduction and the control of gene expression. *Science* **295**: 813–818
- Ghosh S, May MJ, Kopp EB (1998) NF- $\kappa$ B and Rel proteins: evolutionarily conserved mediators of immune responses. *Annu Rev Immunol* **16**: 225–260
- Hoffmann A, Baltimore D (2006) Circuitry of nuclear factor  $\kappa$ B signaling. *Immunol Rev* **210**: 171–186
- Hoffmann A, Levchenko A, Scott ML, Baltimore D (2002) The I $\kappa$ B-NF- $\kappa$ B signaling module: temporal control and selective gene activation. *Science* **298**: 1241–1245
- Ivan M, Kondo K, Yang H, Kim W, Valiando J, Ohh M, Salic A, Asara JM, Lane WS, Kaelin Jr WG (2001) HIF $\alpha$  targeted for VHL-mediated destruction by proline hydroxylation: implications for O<sub>2</sub> sensing. *Science* **292**: 464–468
- Jaakkola P, Mole DR, Tian YM, Wilson MI, Gielbert J, Gaskell SJ, Kriegsheim A, Hebestreit HF, Mukherji M, Schofield CJ, Maxwell PH, Pugh CW, Ratcliffe PJ (2001) Targeting of HIF- $\alpha$  to the von Hippel-Lindau ubiquitylation complex by O<sub>2</sub>-regulated prolyl hydroxylation. *Science* **292**: 468–472
- Karin M (2006) Nuclear factor- $\kappa$ B in cancer development and progression. *Nature* **441**: 431–436
- Kato Jr T, Delhase M, Hoffmann A, Karin M (2003) CK2 is a C-terminal I $\kappa$ B kinase responsible for NF- $\kappa$ B activation during the UV response. *Mol Cell* **12**: 829–839
- Kearns JD, Basak S, Werner SL, Huang CS, Hoffmann A (2006) I $\kappa$ B $\epsilon$  provides negative feedback to control NF- $\kappa$ B oscillations, signaling dynamics, and inflammatory gene expression. *J Cell Biol* **173**: 659–664
- Krappmann D, Wulczyn FG, Scheidereit C (1996) Different mechanisms control signal-induced degradation and basal turnover of the NF- $\kappa$ B inhibitor I $\kappa$ B $\alpha$  *in vivo*. *EMBO J* **15**: 6716–6726
- Lipniacki T, Paszek P, Brasier AR, Luxon B, Kimmel M (2004) Mathematical model of NF- $\kappa$ B regulatory module. *J Theor Biol* **228**: 195–215
- Moon RT (2005) Wnt/ $\beta$ -catenin pathway. *Sci STKE*, **2005**, cm1
- Pando MP, Verma IM (2000) Signal-dependent and -independent degradation of free and NF- $\kappa$ B-bound I $\kappa$ B $\alpha$ . *J Biol Chem* **275**: 21278–21286
- Rice NR, Ernst MK (1993) *In vivo* control of NF- $\kappa$ B activation by I $\kappa$ B $\alpha$ . *EMBO J* **12**: 4685–4695
- Schwarz EM, Van Antwerp D, Verma IM (1996) Constitutive phosphorylation of I $\kappa$ B $\alpha$  by casein kinase II occurs preferentially at serine 293: requirement for degradation of free I $\kappa$ B $\alpha$ . *Mol Cell Biol* **16**: 3554–3559
- Scott ML, Fujita T, Liou HC, Nolan GP, Baltimore D (1993) The p65 subunit of NF- $\kappa$ B regulates I $\kappa$ B by two distinct mechanisms. *Genes Dev* **7**: 1266–1276
- Werner SL, Barken D, Hoffmann A (2005) Stimulus specificity of gene expression programs determined by temporal control of IKK activity. *Science* **309**: 1857–1861
- Yaron A, Hatzubai A, Davis M, Lavon I, Amit S, Manning AM, Andersen JS, Mann M, Mercurio F, Ben-Neriah Y (1998) Identification of the receptor component of the I $\kappa$ B $\alpha$ -ubiquitin ligase. *Nature* **396**: 590–594
- Zandi E, Chen Y, Karin M (1998) Direct phosphorylation of I $\kappa$ B by IKK $\alpha$  and IKK $\beta$ : discrimination between free and NF- $\kappa$ B-bound substrate. *Science* **281**: 1360–1363



*Molecular Systems Biology* is an open-access journal published by *European Molecular Biology Organization* and *Nature Publishing Group*.

This article is licensed under a Creative Commons Attribution License.